Decomposing the effects of ocean warming on chlorophyll *a* concentrations into physically and biologically driven contributions

D Olonscheck[1,2], M Hofmann[1], B Worm[3] and H J Schellnhuber[1,4]

[1] Potsdam Institute for Climate Impact Research, PO Box 601203, D-14412 Potsdam, Germany
[2] Institute for Atmospheric and Climate Science, ETH Zurich, 8092 Zurich, Switzerland
[3] Dalhousie University, Halifax, NS, B3H 4R2, Canada
[4] Santa Fe Institute, Santa Fe, NM 87501, USA

E-mail: Dirk.Olonscheck@pik-potsdam.de

Abstract
Recently compiled observational data suggest a substantial decline in the global median chlorophyll *a* concentration over the 20th century, a trend that appears to be linked to ocean warming. Several modelling studies have considered changes in the ocean's physical structure as a possible cause, while experimental work supports a biological mechanism, namely an observed increase in zooplankton grazing rate that outpaces phytoplankton production at higher temperatures. Here, we present transient simulations derived from a coupled ocean general circulation and carbon cycle model forced by atmospheric fields under unabated anthropogenic global warming (IPCC SRES A1FI scenario). The simulations account for both physical and biological mechanisms, and can reproduce about one quarter of the observed chlorophyll *a* decline during the 20th century, when using realistically parameterized temperature sensitivity of zooplankton metabolism (Q_{10} between 2 and 4) and phytoplankton growth ($Q_{10} \sim 1.9$). Therefore, we have employed and re-calibrated the standard ecosystem model which assumes a lower temperature sensitivity of zooplankton grazing ($Q_{10} = 1.1049$) by re-scaling phytoplankton growth rates and zooplankton grazing rates. Our model projects a global chlorophyll *a* decline of $>50\%$ by the end of the 21st century. While phytoplankton abundance and chlorophyll *a* experience pronounced negative effects, primary production and zooplankton concentrations are less sensitive to ocean warming. Although changes in physical structure play an important role, much of the simulated change in chlorophyll *a* and productivity is related to the uneven temperature sensitivity of the marine ecosystem.

1. Introduction

Ocean ecosystems inherently rely on the net primary production (NPP) of phytoplankton to provide the energetic

base for higher trophic levels. It has been estimated that nearly half of the global NPP is of marine origin (45–50 Pg C yr^{-1}, Falkowski *et al* 1998, Field *et al* 1998), as inferred from the satellite-based Coastal Zone Colour Scanner (CZCS, Feldman *et al* 1989).

Primary production of marine phytoplankton also represents a key component in the oceanic carbon cycle and the Earth's climate system (Behrenfeld and Falkowski 1997). By regulating CO_2 partial pressure (pCO$_2$) and thus

CO_2 air–sea exchange, phytoplankton primary production contributes to the ocean's CO_2 sink (Volk and Hoffert 1985).

Several studies have investigated global trends of phytoplankton concentrations (e.g. Gregg *et al* 2003, 2005, Behrenfeld *et al* 2006, Boyce *et al* 2010, Hofmann *et al* 2011). Therein, the chlorophyll *a* pigment concentration (Chl_a) is commonly used as a proxy for phytoplankton production and biomass. By compiling global annual Chl_a data derived from transparency and direct *in situ* optical measurements, Boyce *et al* (2010) provided a data series from 1899 to 2008 of long-term trends in Chl_a. They discovered declines in eight out of ten ocean regions, and estimated a globally-averaged rate of decline of 0.006 mg m^{-3} yr^{-1}, which represents 1% of the global median Chl_a concentration per year. Physical drivers, especially increased sea surface temperature (SST) and reduced mixed layer depth (MLD), which decrease average nutrient fluxes into the euphotic zone, were suggested as explaining mechanisms. Whereas the large magnitude of observed changes has been questioned (Mackas 2011, McQuatters-Gollop *et al* 2011, Rykaczewski and Dunne 2011), most work supports the conclusion that a warming ocean leads to some decline in average Chl_a, phytoplankton biomass and primary production (Gregg *et al* 2003, Behrenfeld *et al* 2006, Sommer and Lengfellner 2008, Mackas 2011, Boyce *et al* 2011).

To try to test for the physical mechanisms that could potentially elucidate this estimated decline in global phytoplankton, Hofmann *et al* (2011) modelled the impacts of changes in the mixed layer depth (MLD), and, following Schmittner (2005), the strength of the Atlantic Meridional Overturning Circulation (AMOC) on Chl_a and projected future changes under the IPCC's SRES A1FI emission path (Nakicenovic and Swart 2000). The Hofmann *et al* (2011) simulations confirmed the general trend found by Boyce *et al* (2010, 2011), but could not explain the observed magnitude of decline in Chl_a concentrations up to the year 2000. A major decline of up to 50% between 2000 and 2200 is projected by Hofmann *et al* (2011), notably in the North Atlantic and the Arctic Ocean, and largely explained by increasing stratification and changes in deep-water circulation, both of which limit nutrient fluxes into the euphotic zone. They concluded that other mechanisms need to be taken into account to explain the large magnitude of decline observed by Boyce *et al* (2010, 2011).

Both experiments and theory suggest that a biological mechanism may also play a role. Several experiments in temperature-controlled mesocosms have indicated consistent declines in plankton biomass and NPP with increasing warming in winter and spring; these declines were accompanied by declining cell size, and lower dominance by diatoms (Sommer and Lengfellner 2008). These changes are consistent with increased grazing by zooplankton, an explanation which is generally supported by the metabolic theory of ecology (Brown *et al* 2004). According to this theory, metabolic processes such as photosynthesis and respiration are temperature sensitive and are expected to increase at different rates in response to a warming environment. In a recent database analysis, Regaudie-de-Gioux and Duarte (2012) tested the temperature sensitivity

of ocean planktonic communities and identified a two times stronger temperature dependence for community respiration than for gross primary production, a finding consistent with results by Harris *et al* (2006). This indicates lower phytoplankton biomass and a weakening of the CO_2 uptake by phytoplankton with increasing ocean temperatures, and thus a positive feedback between declines in plankton communities and global warming (López-Urrutia *et al* 2006).

Taucher and Oschlies (2011) first modelled direct temperature effects on marine ecosystems due to global warming to detect the direction of change in marine NPP. Their model results show that both the magnitude and direction of NPP change depends on whether metabolic rates are modelled to be temperature dependent or not. Thus, they emphasized the importance of considering temperature sensitivities of metabolic rates when modelling the response of ocean biota to climate change.

This present study investigates the effects of potential drivers on Chl_a concentrations by tracking both changes in physical structure and nutrient supply, while parameterizing for different temperature sensitivities of zooplankton metabolism (Q_{10} between 1.1 and 4.0) and phytoplankton growth ($Q_{10} \sim 1.9$). We decompose the simulated change in Chl_a into a biological and a physical component and calculate their magnitude for the time period between 1800 and 2100 by employing the three-dimensional ocean–atmosphere–sea–ice biogeochemistry model POTSMOM-C (Hofmann and Schellnhuber 2009) forced by the business-as-usual IPCC SRES A1FI emission scenario.

2. Model and experimental design

In the present study we employed the three-dimensional coupled ocean general circulation–sea ice–carbon cycle model POTSMOM-C (Hofmann and Schellnhuber 2009) at a horizontal grid resolution of 3.75° × 3.75°. In this model, the water column is sub-divided into 24 levels with thicknesses increasing from 25 m at the top to ~500 m at the bottom. The ocean part is derived from an improved version (Hofmann and Maqueda 2006) of GFDLs MOM-3 (Pacanowski and Griffies 1999) while the sea ice model by Fichefet and Maqueda (1997) is used. Most notably, the ocean general circulation model (OGCM) benefits from a second-order moments tracer advection scheme nearly free of numerical diffusion and dispersion, allowing the model to run with low vertical background diffusivities on the order of 0.1 cm^2 s^{-1} (Hofmann and Maqueda 2006). The ocean carbon cycle is mainly based on the HAMOCC 3.1 code (Six and Maier-Reimer 1996) which involves a simple nutrient, phytoplankton, zooplankton, detritus (NPZD) model (see Hofmann and Schellnhuber (2009) and Hofmann *et al* (2011) for details). The carbon cycle model is isogeochemical, i.e. chemical weathering and exchange processes with the ocean sediment are not included and it comprises the following prognostic tracers: dissolved inorganic carbon (DIC), total alkalinity, phosphate (PO_4), nitrate (NO_3), dissolved iron (Fe), oxygen

(O$_2$), phytoplankton, zooplankton, particulate organic carbon (POC), dissolved organic carbon (DOC), silicate (SiOH$_4$), and calcite (CaCO$_3$). The Chl$_a$:C ratio of phytoplankton is diagnostically estimated using an empirical relationship to the nutrient concentrations and the photosynthetically available radiation (PAR) and is allowed to vary between 1/37 and 1/90 (Aumont *et al* 2003, Hofmann *et al* 2011).

Following Six and Maier-Reimer (1996), phytoplankton growth rates depend on temperature as described by the Eppley and Peterson (1979) function

$$f(T) = a \cdot b^{cT}, \tag{1}$$

where $a = 0.6$ d^{-1}, $b = 1.066$, and $c = 1.0\,°C^{-1}$ (Six and Maier-Reimer 1996). In terms of the familiar Q_{10} factor, equation (1) can be rewritten as

$$f(T) = a \cdot Q_{10}^{T/10} \tag{2}$$

with $Q_{10} = 1.88$. In accordance with Six and Maier-Reimer (1996), our standard model setup assumes that grazing rates of zooplankton obey the same temperature-dependence law as the growth rates of phytoplankton (equations (1) and (2)), albeit with a lower Q_{10} value of 1.1046. This parameterization was used for the control run in the present paper.

Besides temperature, phytoplankton growth rates strongly depend on the availability and intensity of light. In the ecosystem model employed here, light limitation is parameterized as a function of incoming solar irradiance I (in units of W m^{-2}) and mixed layer depth z (in m)

$$f(I) = I \cdot \alpha \cdot PAR \cdot (1/z) \cdot \int_z dz' \exp\{-kz'\} \tag{3}$$

where k is the light extinction coefficient (0.025 m^2 W^{-1} d^{-1}), PAR = 0.4 the photosynthetically active radiation and $\alpha = 0.03$ d^{-1} m^2 W^{-1} the initial slope of the photosynthetic *P–I* curve (Six and Maier-Reimer 1996).

Numerous mesocosm studies (e.g. Sommer and Lengfellner 2008, Yvon-Durocher *et al* 2010, Sommer and Lewandowska 2011) have suggested a higher temperature sensitivity of zooplankton metabolism and grazing rates compared with phytoplankton metabolism and growth rates. Here we explored the consequences of this discrepancy for marine Chl$_a$ and NPP under an anthropogenic global warming scenario between the years 1800 and 2100. Because we did not run a full-scale atmospheric model, we utilized atmospheric anomalies from previous anthropogenic (A1FI 2100, Nakicenovic and Swart 2000) climate simulations (Kuhlbrodt *et al* 2009) which we superimposed to the NCEP/NCAR reanalysis climatology employed to force our OGCM.

Apart from the standard model described above we have investigated the effects of progressively stronger temperature sensitivities of zooplankton grazing rates on Chl$_a$ levels. We conducted three additional numerical experiments using Q_{10} values of 2.0, 3.0 and 4.0. When evaluating these simulations for the preindustrial state we found an unrealistically large increase in Chl$_a$ in cold polar and subpolar regions and a decline to almost zero in the warm tropics. This phenomenon

Table 1. Implemented scaling factors used to calibrate phytoplankton growth rates, zooplankton grazing rates, and resulting global NPP estimates for different Q_{10} values of zooplankton metabolism.

Q_{10}	Scaling factor zooplankton grazing rate	Scaling factor phytoplankton growth rate	NPP (Pg C yr^{-1})
1.1	1.000	1.000	43.0
2.0	0.800	0.875	39.0
3.0	0.622	0.750	35.5
4.0	0.578	0.625	30.5

can easily be explained by a stronger temperature inhibition of the zooplankton metabolism in cold areas and a stimulated grazing in temperate and warm waters. This leads to pronounced phytoplankton blooms in colder waters, and Chl$_a$ depletion in warm waters. In order to cope with this bias and to enable the models to simulate more realistic Chl$_a$ distribution patterns, it was necessary to re-calibrate the ecosystem model by multiplying the zooplankton grazing and phytoplankton growth rates by a scaling factor (see table 1) in the preindustrial steady state. In doing so we attempted to constrain global marine NPP within the empirically observed range, roughly between 30 and 50 Pg C yr^{-1} (Schneider *et al* 2008). As a result, the modelled NPP for zooplankton Q_{10} values of 1.1, 2.0, 3.0, and 4.0 amounts to 43.0, 39.0, 35.5, and 30.5 Pg C yr^{-1}, respectively (table 1).

We furthermore provided a decomposition of the changes in Chl$_a$ and NPP due to the influence of anthropogenic global warming into a part driven by ocean physics alone and a part caused by increasing zooplankton grazing rates. Therefore we accompanied these model runs with a set of four further simulations, where we drive the ecosystem model with preindustrial temperatures. In other words, while the ocean physics runs under transient anthropogenic forcing, we maintain the temperatures used to derive phytoplankton growth, zooplankton grazing and respiration of organic matter (POC) at preindustrial levels. These latter four 'frozen' model runs provide us with the pure physical effect of global warming, while the difference to the previously mentioned four 'full' simulations defines the biological effect solely caused by different phytoplankton and zooplankton metabolic functions.

3. Results and discussion

After a spin-up time of more than 6000 yr the standard model achieved a quasi-steady state featuring a global NPP of 43.0 Pg C yr^{-1} and a vertical export flux of POC from the upper ocean (100 m horizon) of 8.5 Pg C yr^{-1}, which is comparable to observational data (Schneider *et al* 2008). The model also well reproduced observed large-scale spatial patterns of NPP and surface PO$_4$ concentrations when compared to the data provided by the Sea-viewing Wide Field-of-view Sensor satellite program (SeaWiFS, Behrenfeld and Falkowski 1997) and the field data by Conkright *et al* (1994), respectively (see figure 1). However, the model tended to under-estimate NPP in the subtropical gyres and
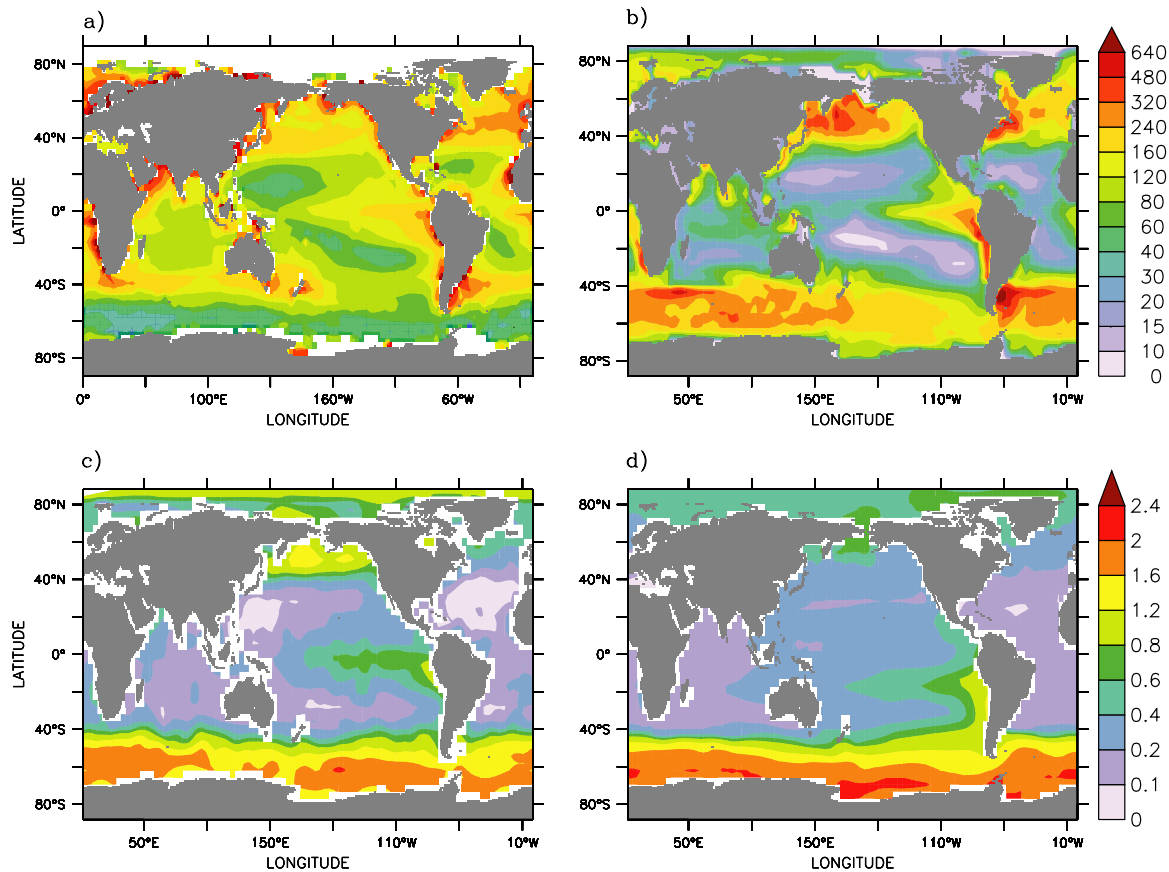
Figure 1. Model comparison with observational data. (a) SeaWiFS-derived NPP field (Behrenfeld and Falkowski 1997); (b) simulated NPP model output in the year 2000; (c) Levitus PO_4 data (Conkright *et al* 1994); (d) simulated PO_4 model output in the year 2000.

revealed higher than observed values in the Southern Ocean (figure 1). A southward-shifted tongue of high surface PO_4 concentrations in the Eastern Tropical Pacific (figure 1(d)) might be the result of an underestimation of the Equatorial upwelling caused by the low vertical background diffusivity in combination with a slow Equatorial current. The simulated global surface Chl_a distribution also resembled the overall spatial pattern of the annual mean values derived from the remotely sensed data (SeaWiFS, Behrenfeld and Falkowski 1997, not shown here), however its absolute values were overestimated by a factor of 2–3, notably in the Southern Ocean. This caveat might be either due to the weakness of the empirical relationship between Chl_a and phytoplankton biomass or due to the fact that the remotely sensed SeaWiFS Chl_a values only represent concentrations in the top surface layer. As an example, optical remote sensing algorithms significantly under-estimate Chl_a concentrations in Antarctic waters for values above around 10 mg m^{-3} (Holm-Hansen *et al* 2004, Korb *et al* 2004, Garcia *et al* 2005, Cunningham *et al* 2011).

Following the SRES A1FI emission scenario, unabated anthropogenic CO_2 emissions were projected to increase to a level of 30 Pg C yr^{-1} in 2100 (see figure 2(a)) leading to about a quadrupling in atmospheric pCO_2 compared to preindustrial values (see figure 2(b)). Consequently, global mean sea surface temperatures (SST) were projected to increase by 6.9 °C until the year 2100 (see figure 2(c)). By influencing

plankton metabolism rates, the increased SST drove changes in marine phytoplankton concentration and thus in NPP.

Forced by global warming, our model simulations investigated the effect of different temperature sensitivities—expressed in terms of Q_{10}—of zooplankton metabolism on Chl_a and NPP levels. Irrespective of the chosen Q_{10} value, all simulations indicated a decline in Chl_a and thus in phytoplankton concentration (figures 2(d)–(e)). While in the standard case of $Q_{10} \sim 1.1$ (black line) Chl_a was projected to drop by 22.5% until year 2100, Q_{10} values of 2.0 (blue line), 3.0 (not shown) and 4.0 (red line) projected a global Chl_a decline by 48.1%, 54.4% and 51.0%, respectively. It is remarkable that even a moderately enhanced Q_{10} of 2.0 led to such a strong decline in Chl_a whereas further enhanced Q_{10} values showed only minor effects. The modelled historic decline in Chl_a reproduced the observed trend during the second half of the 20th century (Boyce *et al* 2010, 2011) when employing a zooplankton $Q_{10} \geq 2.0$, however with a considerably smaller magnitude.

According to our simulations, phytoplankton NPP may decline by 15–20% until 2100 (figure 2(f)), and thus appeared less sensitive to changes in Q_{10} than Chl_a (figure 2(d)). A decomposition of the ecosystem response into a biological and a physical component allows for the comparison of the processes responsible for the relative insensitivity of NPP against changes in Q_{10}. The dashed lines in figure 2(f) indicate the isolated biological component that solely accounts for
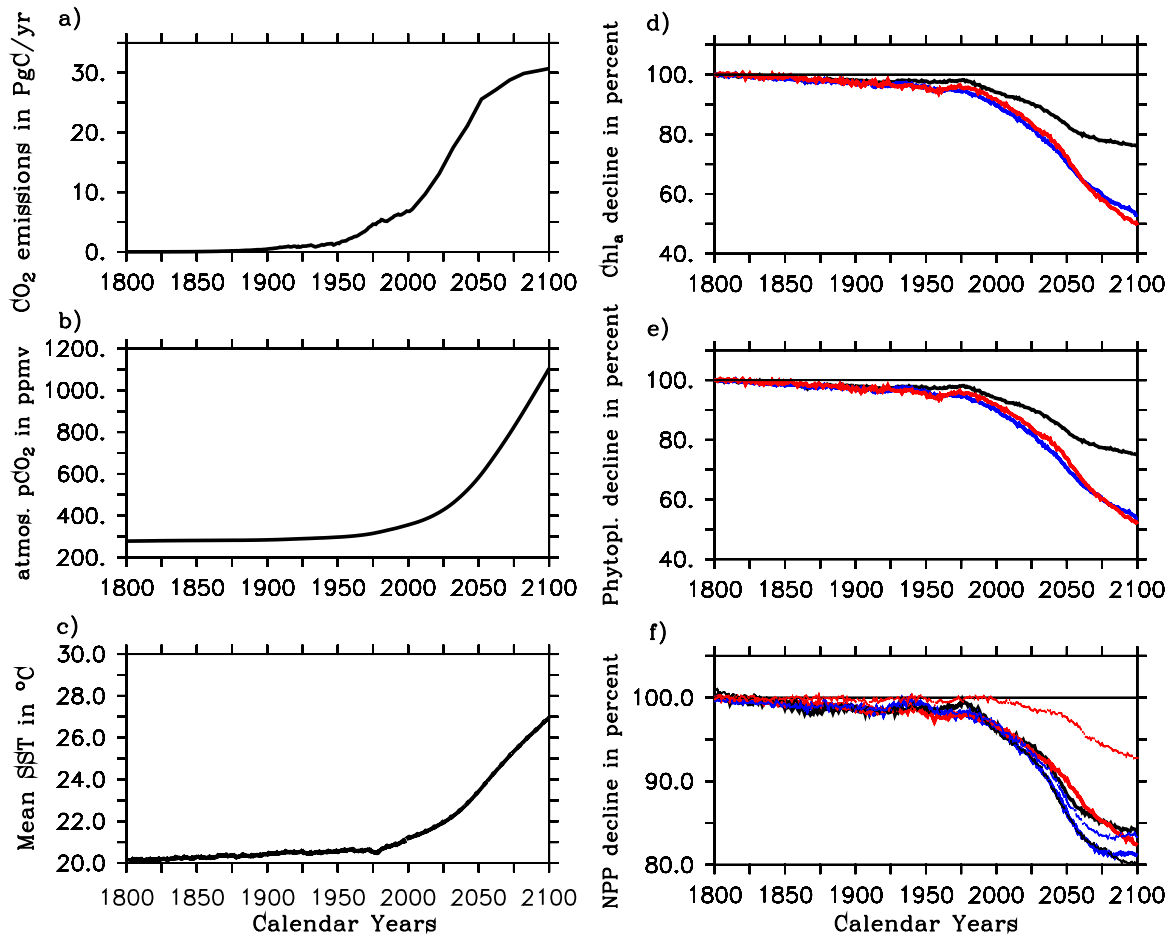
Figure 2. Time evolution of modelled atmospheric and planktonic variables between 1800 and 2100. (a) Anthropogenic CO_2 emissions in Pg C yr^{-1} as projected under SRES A1FI; (b) atmospheric partial pressure of CO_2 (pCO_2) in μatm; (c) mean SST in °C; ((d)–(f)) declines in Chl_a, phytoplankton concentration and NPP in per cent shown for $Q_{10} \sim 1.1$ (black), $Q_{10} = 2.0$ (blue) and $Q_{10} = 4.0$ (red), dashed lines in (f) indicate the biological component of the NPP change that solely accounts for the changes in zooplankton metabolism and the difference to the corresponding solid line represents the physical component.

the changes in zooplankton metabolism. Under $Q_{10} \sim 1.1$ (black dashed line) this biological effect led to a stronger NPP decline compared to the net effect (20.0% versus 16.1% in 2100) as the latter is partly compensated for by changes in physical conditions such as a shrinking of the polar sea ice cover. In contrast, the decline in NPP owing to the temperature dependent metabolic effect was reduced when assuming Q_{10} values of 2.0 and 4.0, respectively (blue and red dashed lines). This is because the photosynthetic production rate increases simultaneously, albeit at a lower rate, with increased community respiration (Brown *et al* 2004, Regaudie-de-Gioux and Duarte 2012), whereby the latter is constrained by respiration of zooplankton (Rivkin and Legendre 2001). Hence, smaller concentrations of phytoplankton are turning over faster at increased ocean temperatures. Owing to the increased excretion of dissolved inorganic matter (DOM) by zooplankton under elevated grazing activities in the model the turnover rate of the microbial loop (Azam *et al* 1983) accelerated, a process also described by Taucher and Oschlies (2011). By capturing the energy transfer and nutrient recycling of DOM via bacteria to higher trophic levels (Azam *et al* 1983, Pomeroy *et al* 2007),

the microbial loop may explain the simulated diminishment of the decline in global NPP when assuming progressively higher zooplankton metabolism temperature sensitivities. Although the response of organic matter fluxes to global change is still uncertain, the flux of DOM shows a large variability (Azam 1998) and recent mesocosm experiments have shown that the partitioning between particulate organic matter (POM) and DOM seems to be highly temperature sensitive, revealing a shift towards DOM at higher temperatures (Wohlers *et al* 2009, Kim *et al* 2011, Taucher *et al* 2012). These experimental results support the assumed enhancement of the microbial loop and are consistent with the finding by Taucher and Oschlies (2011) that changes in NPP are linked to the temperature sensitivity of the microbial loop. They reveal an increase of NPP with higher temperatures when modelling the metabolic processes to be temperature sensitive. Even if our results show a net decline in NPP with an enhanced temperature sensitivity of metabolic processes, which is in accordance with previous studies (Gregg *et al* 2003, Behrenfeld *et al* 2006, Boyce *et al* 2010, 2011, Hofmann *et al* 2011), the direct temperature effects on plankton metabolism cause a weakening of the simulated decline in NPP. If
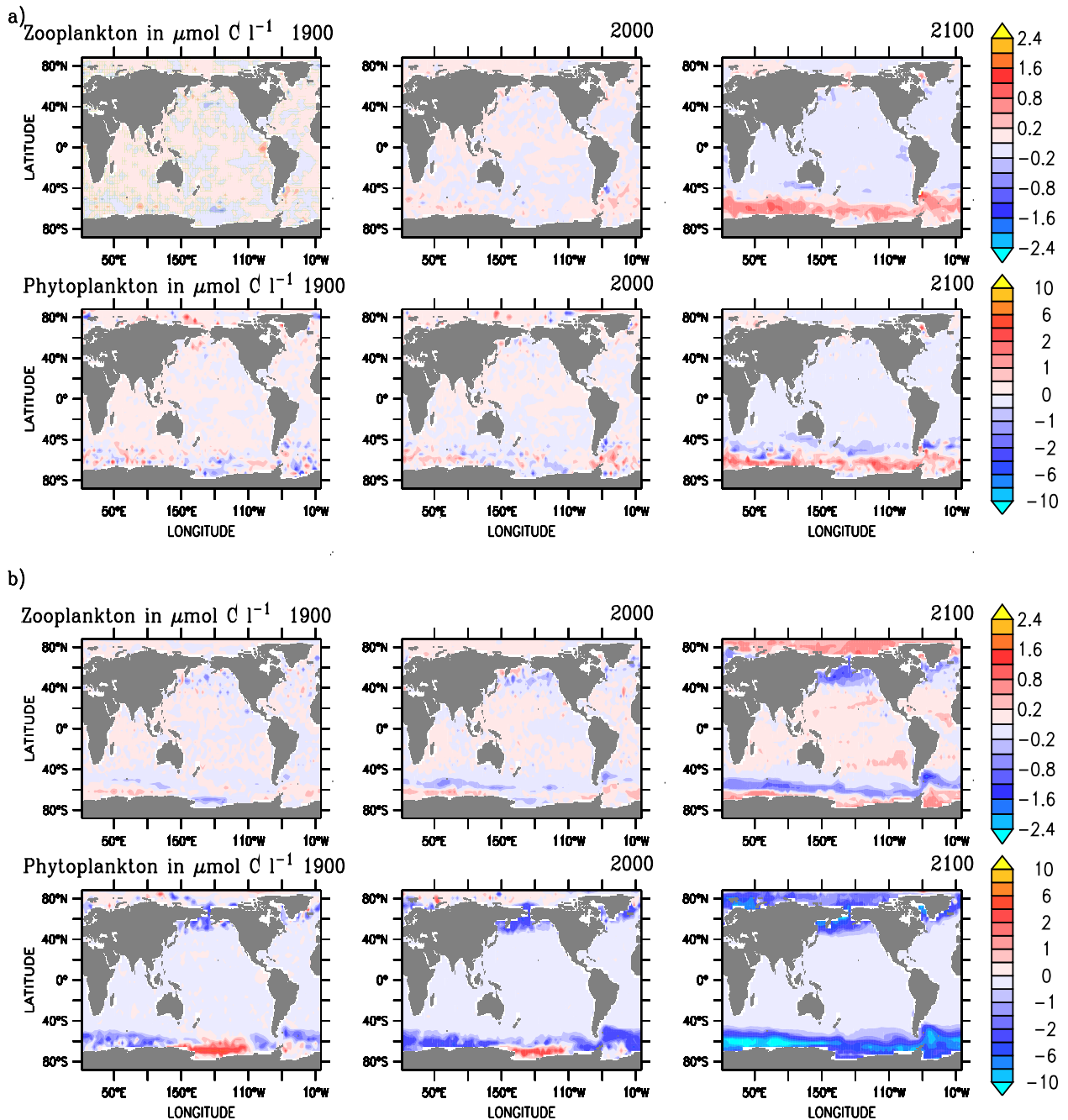
Figure 3. Patterns of change in zoo- and phytoplankton concentrations (μmol C l^{-1}). This is shown for the years 1900, 2000 and 2100 relative to the year 1800 under different temperature sensitivities for zooplankton metabolism, and for the upper 25 m surface layer. Zooplankton metabolic rates are parameterized according to (a) $Q_{10} \sim 1.1$; (b) $Q_{10} = 4.0$. Reddish colours indicate increasing concentrations, whereas bluish and turquoise colours represent decreasing concentrations.

regarded separately, the direct temperature effects are thus attributed to an increase of NPP due to a faster microbial loop. When accounting for changes in physical variables only where metabolic processes are modelled to be insensitive to temperature changes, both our results and the study by Taucher and Oschlies (2011) showed a strong decline in NPP.

For zooplankton, the increasing energy demand for metabolic processes at higher temperatures is satisfied by higher grazing rates. This increased grazing pressure leads to the simulated biologically driven decline in Chl$_a$.

Consequently, the projected global decline in phytoplankton is contrasted by less variable zooplankton concentrations as shown in figures 3(a)–(b). Under a standard $Q_{10} = 1.1046$ only a slight response of both zoo- and phytoplankton is projected for the 21st century with increases in the Southern Ocean and decreases in low and temperate latitudes. As discussed earlier, the model simulations showed a significant decline in phytoplankton concentrations when assuming higher and more realistic temperature sensitivities of zooplankton metabolism ($Q_{10} = 2.0$, 3.0 and 4.0). For
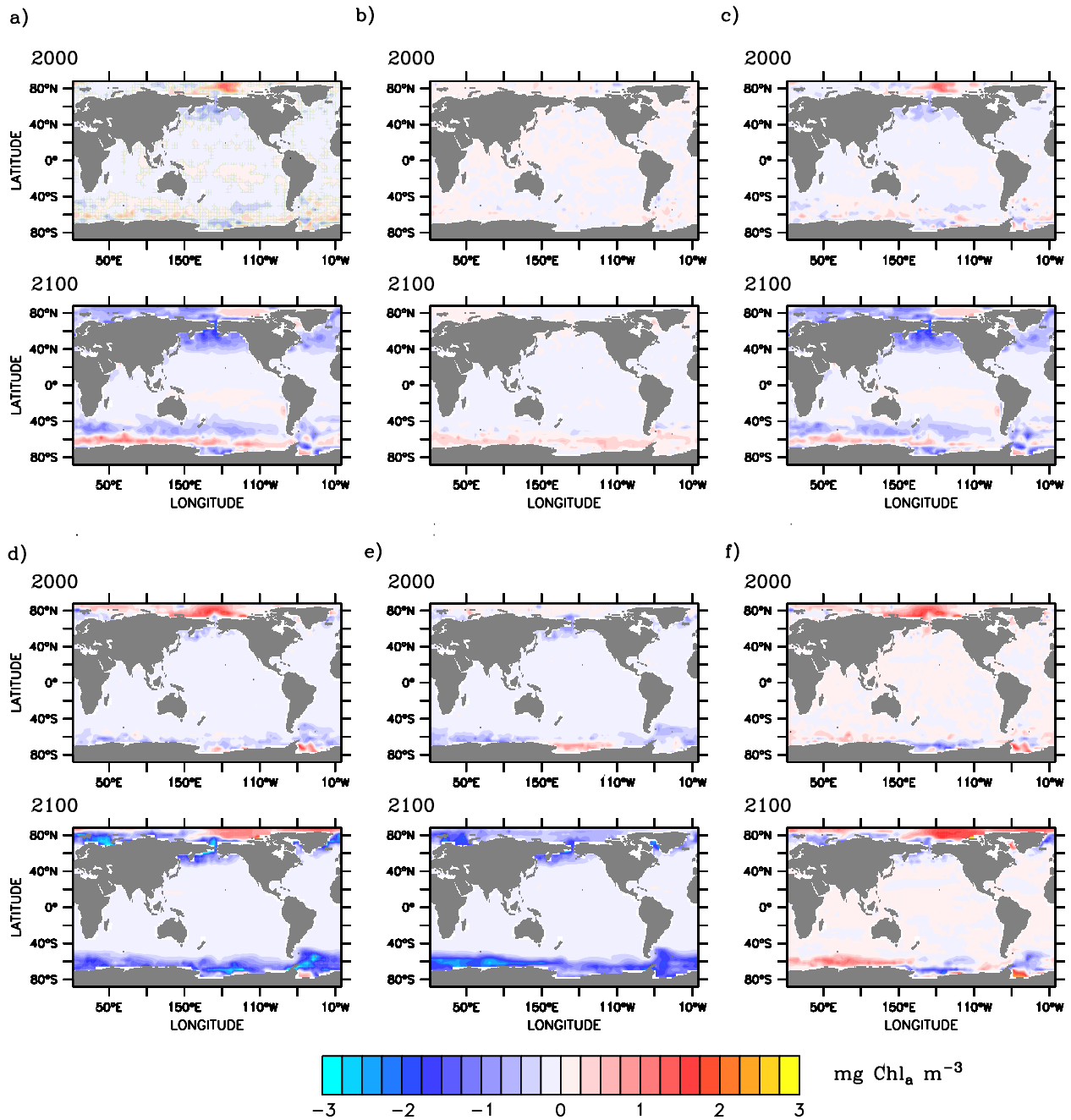
Figure 4. Decomposing the effects of changes in physical structure and plankton metabolism on Chl$_a$. (a), (d) Total simulated Chl$_a$ change in 2000 and 2100 relative to a preindustrial baseline (year 1800), (b), (e) isolated effect of changes in plankton metabolism, and (c), (f) physics, respectively, over the same time frame. Concentrations are expressed in units of mg Chl$_a$ m^{-3} in the upper 25 m ocean layer under different temperature sensitivities for zooplankton metabolism. (a)–(c) $Q_{10} \sim 1.1$; (d)–(f) $Q_{10} = 4.0$. Increases in Chl$_a$ are represented in reddish colours, whereas decreases in Chl$_a$ are shown in bluish colours.

$Q_{10} = 4.0$ the globally-averaged decline in phytoplankton concentrations amounts to 0.21 μmol C l^{-1} (12.1%) until the year 2000 and 0.86 μmol C l^{-1} (48.9%) until the year 2100 (see also figure 2(e)) with a concomitant globally-averaged decrease in zooplankton concentrations of 0.016 μmol C l^{-1} (1.3%) until the year 2000 and 0.065 μmol C l^{-1} (5.7%) until the year 2100, likely in response to the limited availability of phytoplankton. Maximum declines of phytoplankton concentrations of 5.1 μmol C l^{-1} (58.1%) until the year 2100 were projected for the Southern Ocean (ocean region

as defined in Boyce *et al* (2010)). The same patterns of similar magnitudes were projected for $Q_{10} = 3.0$ and 2.0. In these cases, the globally-averaged declines in phytoplankton concentration were 52.2% and 47.1%, respectively.

Our model experiments enabled us to decompose the relative importance of biological mechanisms (plankton metabolism) and physical effects (changes in ocean structure and nutrient supply, figure 4). Assuming a control-run zooplankton Q_{10} of 1.1046 the simulated change in Chl$_a$ was mostly driven by changes in ocean physics (see figures 4(a),

(c)). In general, a shift in Chl$_a$ towards higher latitudes was projected until the year 2100. The increase in Chl$_a$ at high latitudes was mainly due to persistent declines in ocean sea ice cover and increased light availability, whereas the adjacent decreases in subpolar latitudes were linked to temperature-induced changes in ocean physics such as enhanced ocean stratification due to higher SST and thus a diminishment of nutrient supply in surface waters, as discussed by Falkowski *et al* (1998) and Hofmann *et al* (2011). In this standard case, the effects of enhanced grazing are almost negligible (figure 4(b)), and the overall Chl$_a$ decline amounted to 4.8% and 22.5% until the years 2000 and 2100, respectively.

Enhanced Q_{10} values for zooplankton metabolism (Q_{10} = 2.0, 3.0, 4.0) indicated a stronger effect of plankton biology versus ocean physics, as well as much higher rates of decline in global Chl$_a$. Under $Q_{10} = 4.0$ (see figures 4(d)–(f)) the overall effect is described by regional increases in Chl$_a$ in polar latitudes, but a globally-averaged decline in Chl$_a$ of 0.04 mg C m^{-3} (9.0%) until the year 2000 and 0.21 mg C m^{-3} (51.0%) until the year 2100. Here, the biological mechanism was mainly responsible for the projected magnitude of Chl$_a$ decline (figure 4(e)), whereas sea ice melting was projected to cause strong increases in Chl$_a$, notably in the Arctic (see figure 4(f)). The model also showed that while SSTs increased, the summer sea ice cover in both hemispheres began to retreat. As a consequence, the prevailing light limitation of phytoplankton growth was relaxed, allowing for the evolution of phytoplankton blooms. Since zooplankton metabolism was inhibited in the Arctic when imposing a Q_{10} value larger than 2.0, the effects of grazing were negligible. The effect of enhanced temperature sensitivity of zooplankton metabolism completely compensated for increases in Chl$_a$ due to ocean physics and thus explained the projected total declines (figure 4(d)). The globally-averaged contributions to Chl$_a$ change due to ocean physics become secondary under these scenarios (figure 4(f)). Similar patterns were found for $Q_{10} = 4.0$, as for $Q_{10} = 3.0$ and 2.0.

The reason for the relative insensitivity of Chl$_a$ to a doubling of Q_{10} from 2.0 to 4.0 may lie in the nonlinear coupling between phytoplankton and zooplankton. As warmer SSTs stimulate zooplankton growth, Chl$_a$ and phytoplankton concentrations decline. Zooplankton grazing rates, however, also depend on the concentration of phytoplankton described by a Michaelis–Menton term (grazing $\sim P/[P + P_0]$, where P is phytoplankton concentration, $P_0 = 4$ μmol C l^{-1}). This limitation of zooplankton grazing by the concentration of prey (phytoplankton) maintains a considerable Chl$_a$ level in the upper ocean even when imposing higher Q_{10} values for zooplankton metabolism.

The question remains as to which average Q_{10} parameter value should be assumed. Experimental investigations are rare and are confronted with substantial regional and species dependent variability. Only a few studies have analysed the temperature dependence of plankton metabolism. Eppley (1972) calculated a Q_{10} value of 1.88 for both autotrophic and heterotrophic processes. This value has been confirmed by an evaluation of the Eppley function by Bissinger *et al*

(2008) and is widely used in model runs by a number of researchers including Taucher and Oschlies (2011). Six and Maier-Reimer (1996) implemented a relatively low Q_{10} of about 1.1 for zooplankton metabolism in their plankton model integrated in the ocean carbon cycle model HAMOCC3.1. Our standard experiments were based on this code. Several earlier studies assumed a Q_{10} between 2.0 and 2.3 (e.g. Talling 1955, Ichimura 1968, Frost 1987). Recently, the Q_{10} of oceanic plankton metabolism was investigated by Regaudie-de-Gioux and Duarte (2012). Based on a large number of natural communities, they revealed chlorophyll *a*-specific metabolic rates for different oceans. For community respiration, they report a globally-averaged Q_{10} value of about 2.5. According to Ikeda *et al* (2001) the Q_{10} for zooplankton respiration ranges from 1.8 to 2.1, whereas Prosser (1973) reports Q_{10} values for zooplankton filtration rates of 2.0–3.0. Thus, our experiments cover a plausible span of globally-averaged and species-averaged temperature sensitivities of zooplankton metabolism. The assumed Q_{10} of about 1.1 in our standard experiment lies at the low end of reported Q_{10} values, and is likely unrealistic for zooplankton. Taking into account that the average Q_{10} value has important implications for understanding the biological effects of global ocean warming, systematic experimental investigations are needed to determine a reliable globally-averaged value. So far, however, published values between 2 and 4 are projected to have similarly large effects on Chl$_a$ concentrations. The result that both NPP and zooplankton biomass are much less sensitive to warming than the standing stock of phytoplankton is important when discussing possible effects of ocean warming on higher trophic levels. If confirmed, these results may suggest that future marine ecosystems would be supported by similar productivity, and food availability, even at lower average phytoplankton biomass.

4. Conclusions

Our model experiments revealed a progressive decline in phytoplankton Chl$_a$ under a business-as-usual warming scenario. This decline was partly biologically driven (increased grazing rates), and partly physically driven (changes in ocean structure and nutrient supply). We showed that an empirically supported temperature dependence of zooplankton metabolism can lead to remarkable declines in globally-averaged Chl$_a$ concentrations, both in the 20th century (12.1%) and in future projections until the year 2100 (51.0%). Thus, this biological effect may play a significant part in explaining observed declines in Chl$_a$ and should be implemented in future ocean model simulations. Biological mechanisms were dominant relative to changes in physical variables when assuming an average Q_{10} value for zooplankton equal to or greater than 2.0. We conclude that both ocean physics and plankton metabolism may represent major mechanisms to understand observed Chl$_a$ declines. Yet, when taken together these mechanisms can only partly explain published trends in observational data. Our findings especially underline the relevance of the consideration of zooplankton metabolism as an essential part in understanding past and

future evolution of marine biota and thus in understanding the future role of marine phytoplankton in the global carbon cycle.

Acknowledgments

References

Aumont O, Maier-Reimer E, Blain S and Monfray P 2003 An ecosystem model of the global ocean including Fe, Si, P colimitations *Glob. Biogeochem. Cycles* **17** 1060–83

Azam F 1998 Microbial control of oceanic carbon flux: the plot thickens *Science* **280** 694–6

Azam F, Fenchel T, Field J G, Gray J S, Meyer-Reil L A and Thingstad F 1983 The ecological role of water-column microbes in the sea *Mar. Ecol. Prog. Ser.* **10** 257–63

Behrenfeld M J and Falkowski P G 1997 Photosynthetic rates derived from satellite based chlorophyll concentration *Limnol. Oceanogr.* **42** 1–20

Behrenfeld M J, O'Malley R T, Siegel D A, McClain C R, Sarmiento J L, Feldman G C, Milligan A J, Falkowski G P, Letelier R M and Boss E S 2006 Climate-driven trends in contemporary ocean productivity *Nature* **444** 752–5

Bissinger J E, Montagnes D J S, Sharples J and Atkinson D 2008 Predicting marine phytoplankton maximum growth rates from temperature: improving on the Eppley curve using quantile regression *Limnol. Oceanogr.* **53** 487–93

Boyce D G, Lewis M R and Worm B 2010 Global phytoplankton decline over the past century *Nature* **466** 591–6

Boyce D G, Lewis M R and Worm B 2011 Boyce et al reply *Nature* **472** E8

Brown J H, Gillooly J F, Allen A P, Savage V M and West G B 2004 Toward a metabolic theory of ecology *Ecology* **85** 1771–89

Conkright M E, Levitus S and Boyer T B 1994 *World Ocean Atlas 1994, Volume 1: Nutrients, NOAA ATLAS NESDIS 1* (Washington, DC: US Department of Commerce)

Cunningham A, Carrie I and Korb R 2011 Two-component modelling of the optical properties of a diatom bloom in the Southern Ocean *Remote Sens. Environ.* **115** 1434–42

Eppley R W 1972 Temperature and phytoplankton growth in the sea *Fish. Bull.* **70** 1063–85

Eppley R W and Peterson B J 1979 Particulate organic matter flux and planktonic new production in the deep ocean *Nature* **282** 677–80

Falkowski P G, Barber R T and Smetacek V 1998 Biogeochemical controls and feedbacks on ocean primary production *Science* **281** 200–6

Feldman G, Kuring N, Ng C, Esaias W, McClain C, Elrod J, Maynard N, Endres D, Evans R, Brown J, Walsh S, Carle M and Podesta G 1989 Ocean color: availability of the global data set *Eos Trans. Am. Geophys. Union* **70** 634–41

Fichefet T and Maqueda M A M 1997 Sensitivity of a global sea ice model to the treatment of ice thermodynamics and dynamics *J. Geophys. Res.* **102** 12609–46

Field C B, Behrenfeld M J, Randerson J T and Falkowski P 1998 Primary production of the biosphere: integrating terrestrial and oceanic components *Science* **281** 237–40

Frost B W 1987 Grazing control of phytoplankton stock in the open subarctic Pacific Ocean: a model assessing the role of mesozooplankton, particularly the large calanoid copepods Neocalanus supp *Mar. Ecol. Prog. Ser.* **39** 49–68

Garcia C A E, Garcia V M T and McClain C R 2005 Evaluation of SeaWiFS chlorophyll algorithms in the Southwestern Atlantic and Southern Oceans *Remote Sens. Environ.* **95** 125–37

Gregg W W, Casey N W and McClain C R 2005 Recent trends in global ocean chlorophyll *Geophys. Res. Lett.* **32** L03606

Gregg W W, Conkright M E, Ginoux P, O'Reilly J E and Casey N W 2003 Ocean primary production and climate: global decadal changes *Geophys. Res. Lett.* **30** 1809–13

Harris L A, Duarte C M and Nixon S W 2006 Allometric laws and prediction in estuarine and coastal ecology *Estuaries Coasts* **29** 340–4

Hofmann M and Maqueda M A M 2006 Performance of a second-order moments advection scheme in an ocean general circulation model *J. Geophys. Res.* **111** C05006

Hofmann M and Schellnhuber H J 2009 Oceanic acidification affects marine carbon pump and triggers extended marine oxygen holes *Proc. Natl Acad. Sci. USA* **106** 3017–22

Hofmann M, Worm B, Rahmstorf S and Schellnhuber H J 2011 Declining ocean chlorophyll under unabated anthropogenic CO_2 emissions *Environ. Res. Lett.* **6** 034035

Holm-Hansen O *et al* 2004 Temporal and spatial distribution of chlorophyll-a in surface waters of the Scotia Sea as determined by both shipboard measurements and satellite data *Deep-Sea Res. Part II* **51** 1323–31

Ichimura S 1968 Phytoplankton photosynthesis *Algal, Man and the Environment* ed D F Jackson (Syracuse, NY: Syracuse University Press) pp 103–20

Ikeda T, Kanno Y, Ozaki K and Shinada A 2001 Metabolic rates of epipelagic copepods as a function of body mass and temperature *Mar. Biol.* **139** 587–96

Kim J M, Lee K, Shin K, Yang E J, Engel A, Karl D M and Kim H-C 2011 Shifts in biogenic carbon flow from particulate to dissolved forms under high carbon dioxide and warm ocean conditions *Geophys. Res. Lett.* **38** L08612

Korb R E, Whitehouse M J and Ward P 2004 SeaWiFS in the southern ocean: spatial and temporal variability in phytoplankton biomass around South Georgia *Deep-Sea Res. Part II—Top. Stud. Oceanogr.* **51** 99–116

Kuhlbrodt T, Rahmstorf S, Zickfeld K, Vikerbo F, Sundby S, Hofmann M, Link P M, Bondeau A, Cramer W and Jaeger C 2009 An integrated assessment of changes in the thermohaline circulation *Clim. Change* **96** 489–537

López-Urrutia A, San Martin E, Harris R P and Irigoyen X 2006 Scaling the metabolic balance of the oceans *Proc. Natl Acad. Sci. USA* **103** 8739–44

Mackas D L 2011 Does blending of chlorophyll data bias temporal trend? *Nature* **472** E4–5

McQuatters-Gollop A M *et al* 2011 Is there a decline in marine phytoplankton? *Nature* **472** E6–7

Nakicenovic N and Swart R 2000 *IPCC Special Report on Emissions Scenarios* (Cambridge: Cambridge University Press)

Pacanowski R C and Griffies S M 1999 *The MOM-3 Manual, Technical Report* 4 (Princeton, NJ: GFDL Ocean Group/NOAA/Geophysical Fluid Dynamics Laboratory)

Pomeroy L R, Williams P J, Azam F and Hobbie J E 2007 The microbial loop *Oceanography* **20** 28–33

Prosser C L 1973 *Comp. Anim. Physiol.* (Philadelphia: Saunders)

Regaudie-de-Gioux A and Duarte C M 2012 Temperature dependence of planktonic metabolism in the ocean *Glob. Biogeochem. Cycles* **26** GB1015

Rivkin R B and Legendre L 2001 Biogenic carbon cycling in the upper ocean: effects of microbial respiration *Science* **291** 2398–400

Rykaczewski R and Dunne J P 2011 A measured look at ocean chlorophyll trends *Nature* **472** E5–6

Schmittner A 2005 Decline of the marine ecosystem caused by a reduction in the Atlantic overturning circulation *Nature* **434** 628–33

Schneider B, Bopp L, Gehlen M, Segschneider J, Frölicher T L, Cadulen P, Friedlingstein P, Doney S C, Behrenfeld M J and Joos F 2008 Climate-induced interannual variability of marine primary and export production in three global coupled climate carbon cycle models *Biogeosciences* **5** 597–614

Six K and Maier-Reimer E 1996 Effects of phytoplankton on seasonal carbon fluxes in an ocean general circulation model *Glob. Biogeochem. Cycles* **10** 559–83

Sommer U and Lengfellner K 2008 Climate change and the timing, magnitude and composition of the phytoplankton spring bloom *Glob. Change Biol.* **14** 1199–208

Sommer U and Lewandowska A 2011 Climate change and the phytoplankton spring bloom: warming and overwintering zooplankton have similar effects on phytoplankton *Glob. Change Biol.* **17** 154–62

Talling J F 1955 The relative growth rates of three plankton diatoms in relation to underwater radiation and temperature *Ann. Bot. NS* **19** 329–41

Taucher J and Oschlies A 2011 Can we predict the direction of marine primary production change under global warming? *Geophys. Res. Lett.* **38** L02603

Taucher J, Schulz K G, Dittmar T, Sommer U, Oschlies A and Riebesell U 2012 Enhanced carbon overconsumption in response to increasing temperatures during a mesocosm experiment *Biogeosci. Discuss.* **9** 3479–514

Volk T and Hoffert M I 1985 Ocean carbon pumps: analysis of relative strengths and efficiencies in ocean-driven atmospheric CO_2 changes *The Carbon Cycle and Atmospheric CO_2: Natural Variations Archaean to Present* (*Geophys. Monogr. Ser.* vol 32) ed E T Sundquist and W S Broecker (Washington, DC: AGU) pp 99–110

Wohlers J, Engel A, Zollner E, Breithaupt P, Jurgens K, Hoppe H G, Sommer U and Riebesell U 2009 Changes in biogenic carbon flow in response to sea surface warming *Proc. Natl Acad. Sci. USA* **106** 7067–72

Yvon-Durocher G, Jones J I, Trimmer M, Woodward G and Montoya J M 2010 Warming alters the metabolic balance of ecosystems *Phil. Trans. R. Soc.* B **365** 2117–26